Available online at www.sciencedirect.com
ScienceDirect
Journal of the European Ceramic Society 31 (2011) 715–721
www.elsevier.com/locate/jeurceramsoc

Corrosion behavior of ZrO_2–SiO_2–Al_2O_3 refractories in lead silicate glass melts

Rafi Ali Rahimi [a,*], Ali Ahmadi [a], Saeid Kakooei [a], S.K. Sadrnezhaad [b]

[a] *Material Research School, Nuclear Science & Technology Research Institute (NSTIR), Atomic Energy Organization of Iran, Rajaei Shahr, Karaj 31485-498, Iran*
[b] *Department of Materials Science and Engineering, Sharif University of Technology, P.O. Box 11365-9466, Tehran, Iran*

Received 3 November 2010; accepted 24 November 2010
Available online 21 December 2010

Abstract

High-temperature (1200–1350 °C) corrosion of fused-cast ZrO_2–Al_2O_3–SiO_2 (ZAS) refractory contacting lead silicate glass melt (LSG) containing 68.5 wt% PbO was investigated by scanning electron microscopy (SEM), energy dispersive spectroscopy (EDS), differential scanning calorimetry (DSC), x-ray diffraction (XRD), thickness measurement and Archimedes density measurement. ZAS durability was improved by baddeliyete content and deteriorated with open porosity proportion, corundum percentage and eutectic mixture presence. Diffusion of lead resulted in fusion-temperature lowering of the glassy layers embedded within the ZAS particles. Heating caused viscosity drop across the interface, loosening the inter-connected refractory particles and disrupted the crystalline particles residing adjacent to the refractory exterior. Among three ZAS refractories tested in this research, the most durable material was the one with the utmost baddeliyete amount, the least open porosity and the minimum eutectic mixture.

Keywords: ZAS refractory; Corrosion; Lead silicate glass; Diffusion; Glassy phase

1. Introduction

Glass melting tanks require durable refractories resistant to corrosive attack, thermal shock and creep conditions together with small thermal conductivity and controllable thermal expansion coefficient.[1–7] The rate of corrosion reactions that may occur between the refractory and the liquid phase depends on the temperature of the glass melting tank, composition of the melt and porosity of the solid phase. Fused cast ZrO_2–Al_2O_3–SiO_2 (ZAS) refractories are superior because of low porosity, interconnected corundum–baddeleyite particles and interstitial glassy phase.

Lead silicate glass (LSG) has versatile applications in different areas from radiation protection, video-screen manufacturing and glass electrode production to the ophthalmic biotechnology and life science. The lead content of the glass increases the fluidity of the melt and the corrosion rate of the refractory. Difference in constituent chemical potentials of the LSG and the ZAS embedded glass layers produces the driving force for migration of the elements to achieve equilibrium. The migration rate depends on the chemical potential gradient and the binding strength of the elements to their neighbors. Alkali, lead and alkaline earth elements have, for example, small obstacle to the migration. Diffusion of these elements across the interface produces a glassy layer which differs in composition with the ZAS glassy phase and slows down the migration of the diffusing elements.[5–11]

Corrosive effect of the lead silicate glass on refractories has been the subject of many investigations. Pavlovskii et al.,[12] for example, have studied the corrosion of corundum, mullite–corundum and mullite in different lead silicate melts. Corundum offered highest resistance to corrosion in all glass melts; while enhancement of silica decreased the resistance. Duvierre et al.[2] investigated the significance of using the ZAS refractories for production of lead crystal glass. They compared the quality of the glasses produced using both alumina–silicate and the ZAS and found that the ZAS met the present and the future quality requirements of the crystal manufacture. Sedlacek

* Corresponding author. Tel.: +98 261 4464088; fax: +98 261 4464088.
E-mail addresses: rrahimi@nrcam.org (R.A. Rahimi), aahmadi@nrcam.org (A. Ahmadi), skakooei@nrcam.org (S. Kakooei), sadrnezh@sharif.edu (S.K. Sadrnezhaad).

0955-2219/$ – see front matter © 2010 Elsevier Ltd. All rights reserved.
doi:10.1016/j.jeurceramsoc.2010.11.022

Table 1
Chemical composition, mineral analysis and physical properties of the refractories used in this research.

Sample	Composition						
	ZrO_2	Al_2O_3	SiO_2	Na_2O	CaO	TiO_2	Fe_2O_3
Chemical analysis (wt%)							
ER	32.5 ± 1	50.9 ± 2	15 ± 0.5	1.3 ± 0.1		0.3 ± 0.0	
CS-3	34.5 ± 1	48.0 ± 2	15 ± 0.5	1.5 ± 0.1		0.2 ± 0.0	
CS-4	37.2 ± 1	47.0 ± 2	14.2 ± 0.5	1.5 ± 0.1		0.2 ± ±0.0	

Sample	Phase		
	Corundum	Baddeleyite	Glass
Mineral analysis (wt%)			
ER	47 ± 1	32 ± 1	21 ± 1
CS-3	47 ± 1	33 ± 1	20 ± 1
CS-4	46 ± 1	36 ± 1	18 ± 1

Sample	Property	
	Density (g/cm^3)	Porosity (%)
Physical properties		
ER	3.80 ± 0.2	0.51 ± 0.1
CS-3	3.78 ± 0.2	0.77 ± 0.1
CS-4	3.79 ± 0.2	1.15 ± 0.1

et al.[6] studied corrosion of the ZAS refractories contacting lead crystal glass melts. They concluded that the diffusion of the metal ions of the lead glass into the glassy phase of the refractory originated the corrosion. Verlotski et al.[13] investigated the corrosion of the ZAS and some ceramic based Cr_2O_3 refractories contacting silicate glasses containing high and low lead content. They found that the ZAS had relatively good chemical durability.

In spite of all the above investigations, the effects of formation of the secondary glassy layer and its microstructure on corrosion behavior of the ZAS refractories contacting the LSG melts have not yet been thoroughly elucidated. Present study considers the corrosion of fused cast ZAS refractories contacting the LSG melts of different temperatures. SEM, XRD, STA and EDS techniques were employed to characterize the products of the corrosion process.

2. Experimental procedure

Fused cast ZAS refractories "Cs-3", "Cs-4", Monofrax and ER1681 of France with specifications given in Table 1 were used in this research. Open porosities were measured by immersing refractory samples into deionized water and weighing with Mettler Toledo AG204 balance having ±0.0001 g accuracy. The refractory probes were cut by a diamond saw into $0.01 \times 0.01 \times 0.05\ m^3$ rectangular blocks and dipped into liquid lead silicate glass for determination of their corrosion rate.

Technical grades silica >99.9 (Iran, Hamedan), Pb_3O_4 (Iran) and reagent grades Na_2O, K_2O, ZrO_2, TiO_2 and As_2O_3 (Aldrich Chemical Co.) were melted in several alumina crucibles to produce LSG samples weighing 0.5 Kg and containing PbO (68.5 wt%), SiO_2 (24 wt%), ZrO_2 (2.4 wt%), TiO_2 (1 wt%), Al_2O_3 (2.2 wt%), Na_2O (1.6 wt%) and As_2O_3 (0.3 wt%) constituents. Electric furnace (Exciton Co., Iran) was used to melt the samples and keep them at 1200–1300 °C for 2 h under atmospheric conditions. Glass melts were quenched in water and then ground in a ceramic mortar.

The corrosion of the ZAS refractory immersed in the LSG melt was carried out according to the ASTM C-621[14] standard. Refractory probes were hung from alumina cap into the LSG frit charged into alumina crucibles, as indicated in Fig. 1. The crucibles were heated simultaneously by the electric furnace to obtain the different pre-determined temperatures (1200, 1250, 1300 and 1350 °C) under the atmospheric pressure. The set-up was maintained for 100 h at the specified temperatures. The crucibles were pulled-out of the furnace at the end of each experiment. The refractory probes were removed from the LSG melt and laid down on alumina substrates sitting within the furnace chamber. The furnace was turned off and the probes were cooled down to the room temperature.

Corroded refractory probes were cut into small pieces with diamond saw for characterization purposes. Relative reduction in the refractory thicknesses was evaluated from the following correlation:

$$L_R = \frac{(L - l) \times 100}{L}.$$

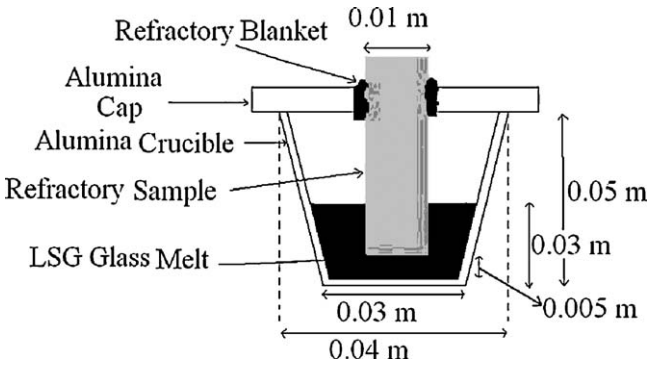

Fig. 1. Schematics of the experimental setup used for corrosion measurements.[8]

Table 2
Chemical compositions of the matrix glassy phases of the refractories before corrosion tests.

Sample	Composition		
	SiO_2	Al_2O_3	Na_2O
ER			
wt%	51.8 ± 5.0	37.8 ± 7	10.5 ± 1.5
mol%	60.5 ± 5.9	26.2 ± 4.9	12.5 ± 1.8
CS-3			
wt%	55.7 ± 3.6	39.7 ± 4.0	4.5 ± 0.6
mol%	66.5 ± 4.2	28.1 ± 2.8	5.3 ± 0.7
CS-4			
wt%	64.8 ± 0.9	28.9 ± 0.8	6.3 ± 0.1
mol%	73.9 ± 1.0	73.9 ± 1.0	6.9 ± 0.1

Where "L_R" is the relative thickness reduction, "L" is thicknesses of the specimen before the corrosion test and "l" is thicknesses of the specimen after the corrosion test measured from their cut face. Mean thickness reductions were determined via five independent measurements.

The preceding glassy phase of the ZAS refractory contained SiO_2, Al_2O_3 and Na_2O oxides (Table 2). From Al_2O_3–SiO_2–Na_2O equilibrium ternary diagram, the melting point of the glassy layer was determined. The points highlighted on the diagram indicated the chemical composition of different refractory materials used in this research (Table 2).

Three glassy samples were prepared with the same compositions as that of the glass layers formed on the surface of the ER, Cs-3 and Cs-4 refractory probes during the corrosion tests (Table 4). Transition temperatures of these layers were determined by Rheometric Scientific, STA 1500 thermal analyzer. Scanning rate of temperature was 10 °C/min raising from ambient to 1400 °C under flowing dry air.

Microstructure, elemental analyses and crystalline phases of the refractory probes before and after corrosion tests conducted at 1350 °C were determined by scanning electron microscopy (Philips, XL30) equipped with energy dispersive spectroscopy (EDS) and x-ray diffractometry (XRD, Philips, PW 1800, Cu Ka radiation).

3. Results and discussion

Chemical composition of the initial glassy phase is summarized in Table 2. SEM micrographs of the un-corroded refractory probes are shown in Fig. 2 highlighting baddeleyite (B), corundum (C), near-eutectic Al_2O_3–ZrO_2 mixture (E: fine zirconia and corundum crystals mixture) and the initial glassy phase (G). Fig. 3 shows the EDS pattern of the baddeleyite, the corundum and the eutectic mixture (E) recognized by elemental analysis of the surface layer of the ZAS. The relative reduction in the refractory mean thicknesses at different temperatures is illustrated in Table 3.

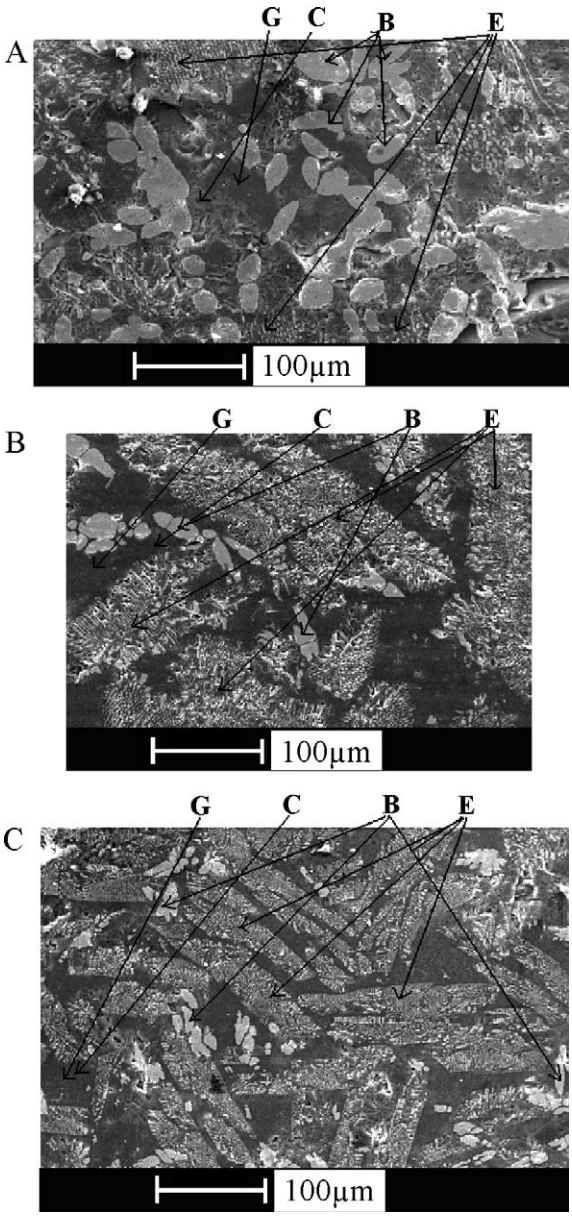

Fig. 2. SEM micrographs of the: (a) ER, (b) CS-3 and (c) CS-4 refractories before corrosion tests: B, baddeleyite; C, corundum; E, Al_2O_3–ZrO_2 laths near eutectic structure; and G, glass matrix.

Table 3
Relative thickness reduction of the "ER", the "Cs-3" and the "Cs-4" refractories after corrosion tests conducted at different temperatures.

Refractory prob.	Temperature (°C)			
	1200	1250	1300	1350
ER	0.70 ± 0.03	1.06 ± 0.09	1.88 ± 0.04	3.96 ± 0.13
Cs-3	0.94 ± 0.07	3.76 ± 0.05	5.42 ± 0.04	6.12 ± 0.17
Cs-4	2.62 ± 0.06	6.30 ± 0.07	12.62 ± 0.12	17.92 ± 0.17

SEM micrographs of the cross-section of the corroded refractory probes are shown in Fig. 4. Table 4 indicates the chemical composition of the secondary glassy layer. Diminution of both silica and alumina contents concomitant with presence of the incoming lead are inspected at the surface of the corroded ZAS. The formation of a new glassy phase in the superficial layer of the ZAS is, therefore, assessed.

Table 4
Chemical composition of secondary glass phases produced on surface of the "ER", the "Cs-3" and the "Cs-4" refractories after corrosion tests conducted at 1350 °C.

Sample	Composition			
	SiO_2PbO	PbO	Al_2O_3	Na_2O
ER				
wt%	37.0 ± 3.6	37.9 ± 4.5	19.7 ± 1.8	5.4 ± 0.4
mol%	57.7 ± 5.6	15.9 ± 1.9	18.2 ± 1.7	8.2 ± 0.6
Cs-3				
wt%	32.5 ± 2.5	43.0 ± 4.5	18.4 ± 3.2	6.1 ± 0.6
mol%	53.6 ± 4.1	18.8 ± 2.0	17.8 ± 3.1	9.8 ± 1.0
Cs-4				
wt%	32.0 ± 1.4	45.8 ± 3.0	16.3 ± 2.2	5.9 ± 0.6
mol%	53.5 ± 2.3	20.0 ± 1.3	16 ± 2.2	10.5 ± 1.1

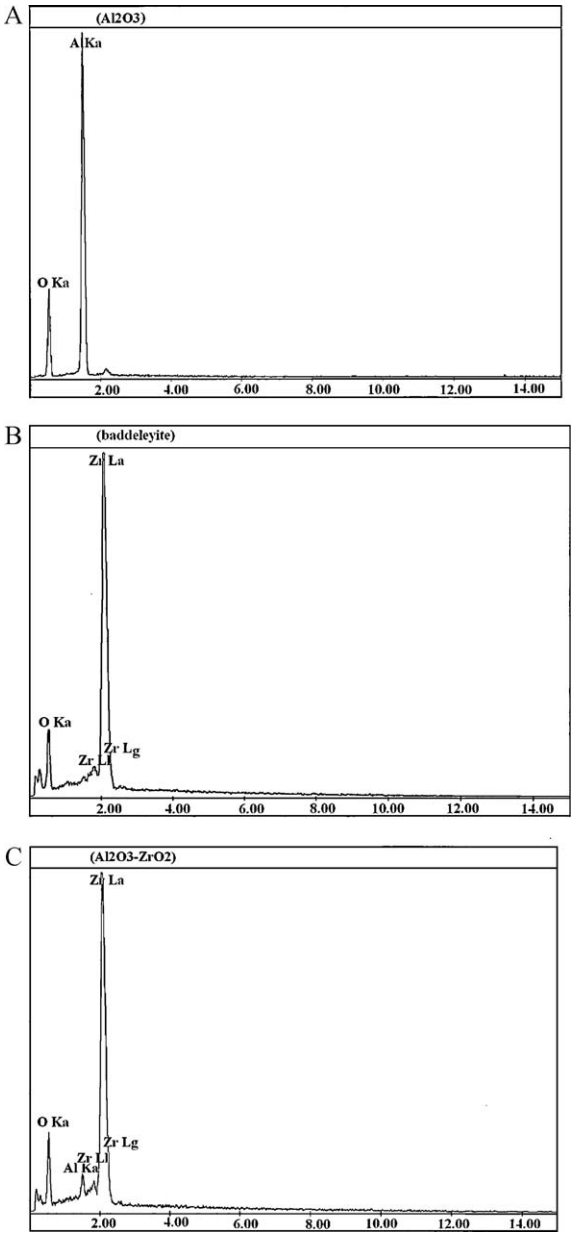

Fig. 3. EDS patterns of (a): Al_2O_3 (corundum), (b): ZrO_2 (baddeleyite) and (c): Al_2O_3–ZrO_2 (eutectic mixture) particles indicated in Fig. 2.

The melting temperature of the secondary glassy phase significantly influences the corrosion rate of the ZAS. The melting temperatures of the preceding ZAS glassy phase estimated from the ternary phase diagram of the Al_2O_3–SiO_2–Na_2O_3 system, shown in Fig. 5. The melting temperature of the secondary glassy phase is measured by thermal analysis (Fig. 6). All values are highlighted in the ternary phase diagram, as illustrated in Fig. 5. The melting ranges are estimated from the isothermal

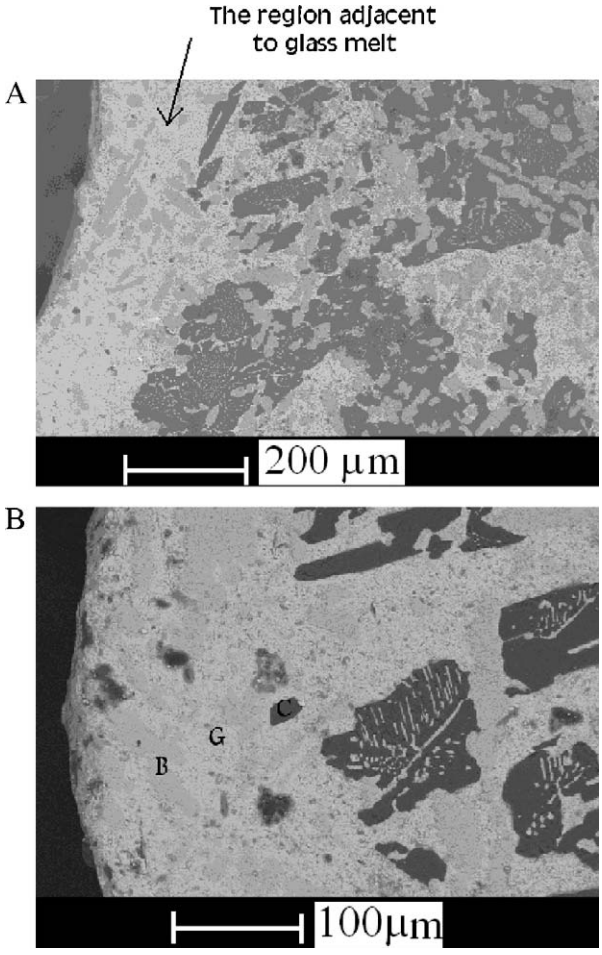

Fig. 4. SEM micrographs of Cs-3 cross-section corroded with the LSG melt at 1350 °C taken from a region adjacent to the LSG melt: (a): lower magnification and (b): higher magnification.

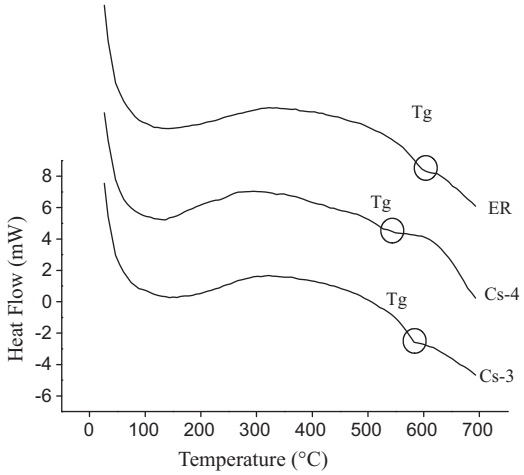

Fig. 5. DSC pattern of the secondary glassy phases produced at the surface of the "ER", the "Cs-3" and the "Cs-4" refractories during the corrosion tests.

best fit lines of the highlighted points. These temperatures are estimated above 1600 °C. The range of the T_g values (Fig. 5) indicates that all the secondary glassy phases are molten during the experiments. The viscosity of the secondary glassy phase is thus situated between that of the LSG and the initial glassy phase.

Formation of the secondary glassy phase significantly influences the corrosion of the ZAS. Contact of the LSG melt with the ZAS refractory results in migration of the attacking elements such as lead. Diffusion coefficient of the migrating element depends on the temperature. Mobility and passed over distances increase by temperature. Diffusion continues until the glassy boundary layer saturates. At the glassy boundary layer, the migrating element occupies a new chemical state. The thickness of the glassy boundary (secondary) layer depends on the migration distance of the diffusing element into the glassy phase which enhances with temperature. Presence of lead considerably reduces the melting temperature of the secondary glassy phase well below the initial glassy phase of the ZAS.

Corrosion of the ZAS refractory in the LSG melt is carried out by detaching of the refractory particles (baddeleyite, corundum and eutectic mixture) adhered to each other by the glassy phase. At higher temperatures, viscosity decreases loosening connections between particles. Particle detachments are induced by mechanical forces facilitating their entrance into the LSG melt. Further content change of the secondary layer causes more ZAS disruption.

Chemical reactions speed up with the surface area of the LSG/ZAS interface. Open porosity and interface surface area of the ER probe is lower than the others. Zirconia content also influences the chemical durability of the ZAS. Previous authors have demonstrated that zirconia[6,9,15] can improve chemical durability against dissolution of various glass melts. This material appears in two microstructural forms of baddeleyite (B) and eutectic mixture (E) which significantly influence the ZAS

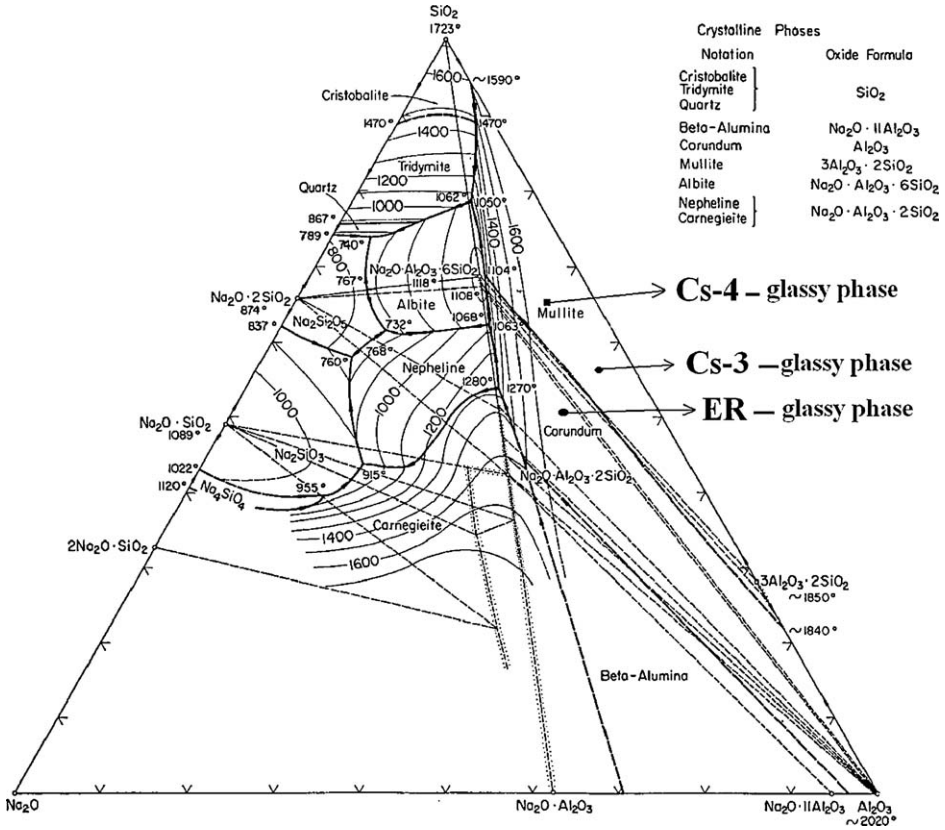

Fig. 6. Ternary phase diagram of Na_2O–Al_2O_3–SiO_2. The spots marked with (■), (♦) and (●) indicate chemical composition of the preceding glassy phase on surface of the Cs-4, the Cs-3 and the ER refractories, respectively.

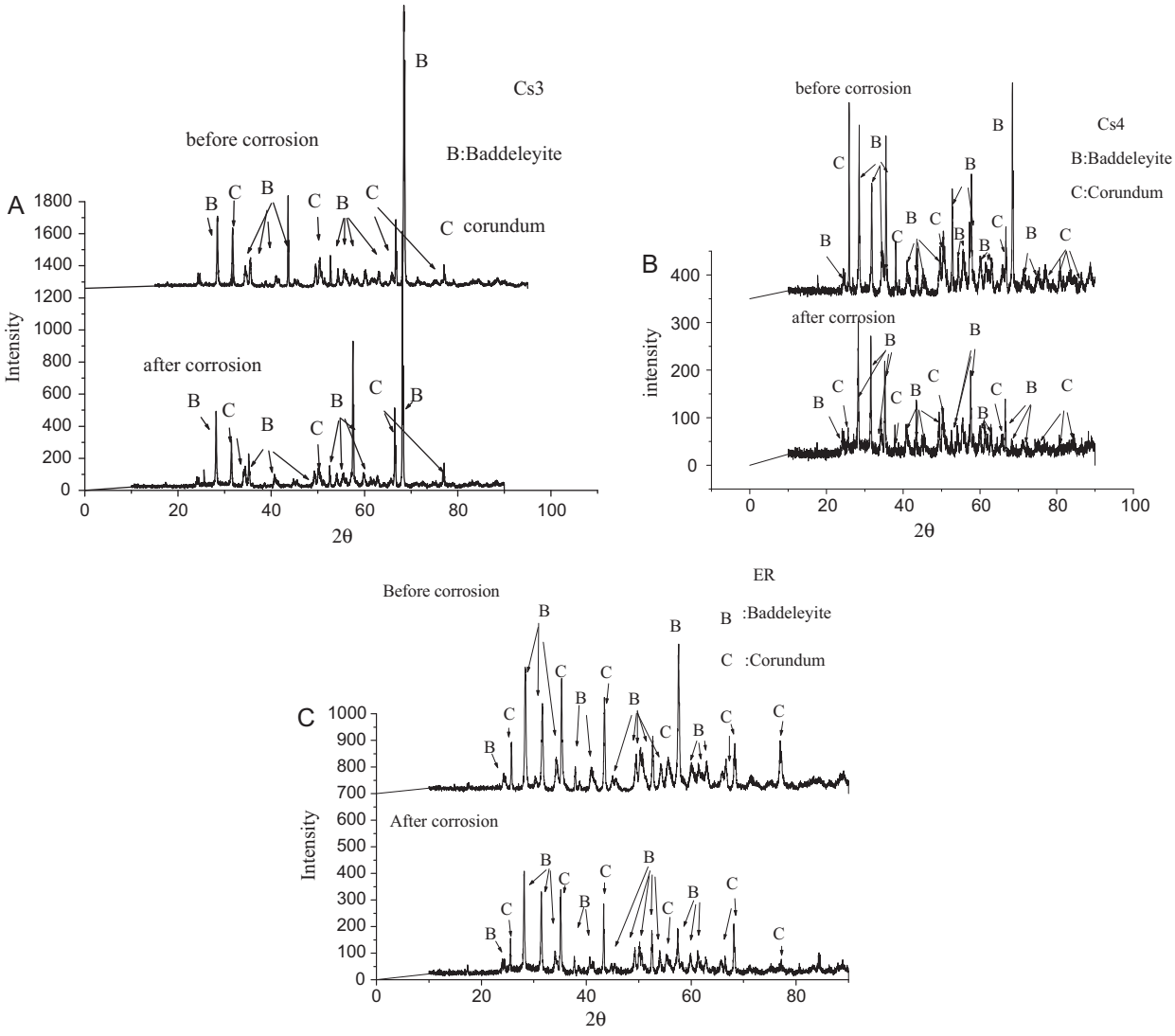

Fig. 7. The XRD patterns of the unused and corroded refractories.

chemical durability.[15] Cs-4 and Cs-3 refractory probes contain, for example, mostly eutectic mixture; but ER refractory includes baddeleyite particles. The experimental and analytical results show that ER presents better chemical durability than the Cs-4 and Cs-3 samples (Table 3).

The chemical durability of the eutectic mixture depends on behaviors of the two components (i.e. corundum and zirconia). It is obvious from the SEM micrographs (Figs. 2 and 4) that the zirconia phase has porous structure. Due to its poor chemical durability, corundum dissolves first into the liquid LSG phase. This produces a relatively large amount of contact area between the glassy phase and the zirconia particles. This process together with the mechanical forces caused detachment of the zirconia particles and expedited the corrosion procedure. The dense structure of the baddeliyete particles displays, however, an extremely small interface between zirconia and the glassy melt. Superior chemical durability and lack of strong mechanical forces cause negligible disruption of the refractory material adjacent to these particles.

Another factor which influences the chemical durability of the refractory materials is the size of the eutectic particles. Both Cs-3 and Cs-4 samples contain, for example, approximately the same amount of the eutectic mixture; while the lower size of the eutectic particles causes larger contact areas and relatively lower chemical durability of the Cs-4 probe as compared to that of the Cs-3 probe.

Fig. 7 shows the XRD patterns of the different refractory probes before and after corrosion experiments. In all refractory probes (corroded and un-corroded), it is observable that the diffraction peaks appear at the same 2θ angles; while relative intensities of the individual peaks are not the same. The XRD patterns of all refractory probes indicate the presence of the baddeleyite and the corundum phases. While they show no other crystalline phases in the unused and the corroded refractory samples. The patterns clearly show intensity reduction in the baddeleyite and corundum peaks after the corrosion tests.

The SEM micrographs (Fig. 4) and the EDS analyses (Table 4) of the refractories verify partial dissolution of the

corundum particles into the glassy boundary layer; but they do not show any dissolution of the baddeleyite phase. Permeation into the refractory porosities of the LSG melt together with the formation of the Pb-rich glassy boundary layer causes the increase of the weight percent of the glass constituents of the refractory sample. Due to this phenomenon, the concentration of the baddeleyite phase adjacent to the surface layer of the refractory probe reduces and the intensity of the corresponding peaks becomes lower. Intensity reduction of the corundum peaks is also related to the dissolution of the corundum into the secondary glassy phase and the glass phase enhancement of the ZAS sample.

4. Conclusion

Diffusion of lead into the interface layer of the ZAS refractory produces a secondary glassy phase adjoining to the LSG melt. Due to its higher modifier content, the glassy boundary layer has lower viscosity than the preceding parent refractory sample especially at the high corrosion temperatures. Temperature increases both diffusion affected zone of the modifying cations and the thickness of the created secondary glassy phase. Lowering with temperature of the boundary layer viscosity causes loosening of the refractory particles (baddeliyete and eutectic mixture) initially adhered to the ZAS with the help of the penetrating glassy phase. Due to this phenomenon and presence of the mechanical forces, the refractory particles are disrupted from one another and from the ZAS to freely enter into the LSG melt. ZAS durability increases, hence, by the baddeleyite content and decreases by the open pore percentage, eutectic ratio, corundum content and the working temperature. The ER refractory shows the highest chemical durability of three refractories investigated in this research.

References

1. Velez M, Smith J, Moore RE. Refractory degradation in glass tank melter: a survey of testing methods. *Ceramica* 1997;**43**:178–82.
2. Duvierre G, Stertain E, Reber A. Advantages of using high zirconia refractories in lead crystal glass electric furnaces. *Glass Technology* 1993;**34**:181–6.
3. Li H, Cheng J, Tang L. Corrosion of electrocast AZS refractories by CAS glass–ceramics melting. *Journal of Non-Crystalline Solids* 2008;**354**:1418–23.
4. Aksel C, Dexet M, Logen N, Porte F, Riley FL, Konieczny F. The influence of zircon in a model aluminosilicate glass tank forehearth refractory. *Journal of European Ceramic Society* 2003;**23**:2083–8.
5. Spear KE, Allendort MD. Thermodynamic analysis of alumina refractory corrosion by sodium or pottasium hydroxide in glass melting furnaces. *Journal of Electrochemical Society* 2002;**149**:B551–9.
6. Sedlacek J, Jamnicky M, Lokaj J. Microstructural analysis and properties of fused cast zirconia refractories corroded in lead glass. *Solid State Phenomena* 2003;**90–91**:253–8.
7. Dunki M. *Glass melt–refractories interaction, a report of VESUVIUS Glass group*. Germany: Dusseldorf; 2001.
8. Dunki M. Corrosion of refractories by glass melts and suggestions for the reduction of the corrosion rate. In: *UNITCER 91*. 1991. p. 413–5.
9. Bieler BH. Corrosion of AZS, zircon, and silica refractories by vapors of NaOH and of $NaCO_3$. *Ceramic Bulletin* 1982;**61**:746–9.
10. Vázquez BA, Pena P, de Aza AH, Sainz MA, Caballero A. Corrosion mechanism of polycrystalline corundum and calcium hexaluminate by calcium silicate slags. *Journal of European Ceramic Society* 2009;**29**:1347–60.
11. Balikoglu F, Akkurt S. Isothermal corrosion testing of frit furnace refractories. *Ceramics International* 2009;**35**:3411–9.
12. Pavlovskii VK, Sobolev YS. Corrosion of refractory materials in molten lead–silicate glasses. *Glass and Ceramics* 1992;**49**:367–9.
13. Verlotski AA, Rublevskii IP, Kulikova MV, Frolova VP. Resistance of refractories to lead glass melts. *Glass and Ceramics* 1985;**42**:182–6.
14. *Standard test method for isothermal corrosion resistance of refractories to molten glass*. ASTM C-621; 1999. p. 157–62.
15. Manfredo LJ, Mcnally RN. The corrosion resistance of high ZrO_2 fusion-cast Al_2O_3–ZrO_2–SiO_2 glass refractories in soda lime glass. *Journal of Materials Science* 1984;**19**:1272–6.